MEMBER REPORT

[*China*]

ESCAP/WMO Typhoon Committee
16th Integrated Workshop
(Video conferencing)
2-3 December 2021

CONTENTS

I. Review of Tropical Cyclones Affecting China since Last Session of ESCAP/WMO Typhoon Committee

1.1 Meteorological and Hydrological Assessment

From August 2020 to March 2021, a moderately intense eastern type La Nina event occurred in the equatorial Middle Eastern Pacific. This caused the prevailing cyclonic circulation anomaly in the lower troposphere over the northwest Pacific (NWP) in the spring and summer of 2021 and the subtropical ridge to drift northward. Which are favorable for tropical cyclone genesis and northward moving tracks. An anomalous anti-cyclonic circulation has occurred over NWP since August 2021, with strengthened and westward stretched subtropical high. The convection in the western Pacific warm pool was inhibited and the monsoon trough was abnormally weak, which was unfavorable for tropical cyclone genesis.

From 1 January to 15 November, 2021, the NWP and the SCS have witnessed the generation of 20 Tropical Cyclones (TCs), which is 3.4 less than the average number (23.4) of multiple years. Among those 20 TCs, Severe Typhoon IN-FA (2106), Typhoon CEMPAKA (2107), Tropical Storm LUPIT (2109), Tropical Storm LIONROCK (2117) and Typhoon KOMPASU (2118) made landfall on the coastal area of China. It is 1.9 less than the average number (6.9) of multiple years.

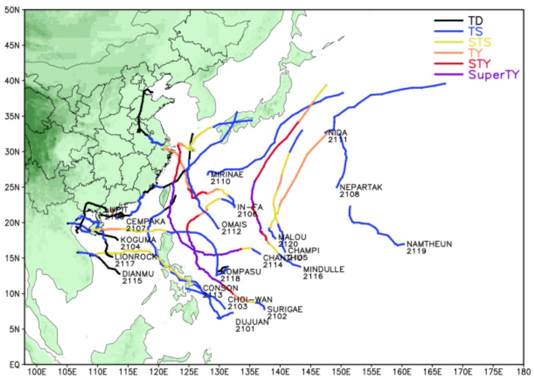

Fig. 1.1 Tracks of TCs over the NWP and the South China Sea from 1 January to 15 November 2021

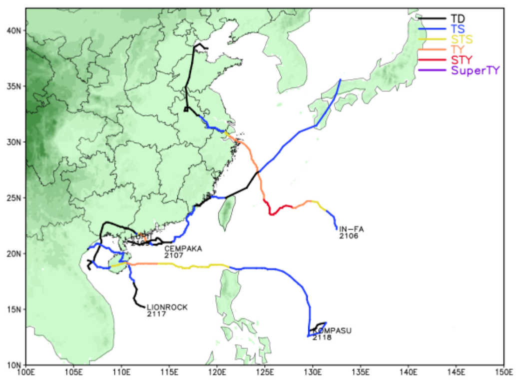

Fig1.2 Tracks of TCs that made landfall over China from 1 January to 15 November 2021

1.1.1 Characteristics of TCs in 2021

The characteristics of typhoons in 2021 are as follows: the source area of typhoons is north and west, the number of typhoons and landings is less, and the peak intensity and landings intensity are weak.

1) Westward and Northward Origins

Up to November 15th 2021, the averaged genesis location of the 20 TCs is 17.4°N, 131.2°E, which are 1.3 latitude to the north and 5.2 longitude to the west compared with the annual average (16.1°N, 136.4°E) (Figure 1.3).

2) Fewer TC Genesis with Lower Intensity

Up to November 15th 2021, there were totally 20 TCs generated in the NWP and the South China Sea (SCS), 3.4 less than the average; the average peak intensity of the totally 20 TCs is 32.3m/s, which is significantly weaker than that of multiple years (40.1m/s). Usually, 38.8% of the total numbers of typhoons in the year are at or above the severe typhoon grade. While in 2021, there are only 3 TCs stronger than severe typhoon during their lifetimes, accounting for only 15.0% of the total. The intensity of TCs in this year is obviously weaker than usual.

3) Concentrated Time and Cluster of TCs' Genesis

Up to 15 November 2021, of the 20 TCs, only 7 were active alone, while others appeared as binary or triple TCs. There are two triple-typhoons events occurred. The first one is LUPIT, MIRINAE and NIDA. The second is LIONROCK, KOMPASU and NAMTHEUN. On average, there are only1.5 such events per year.

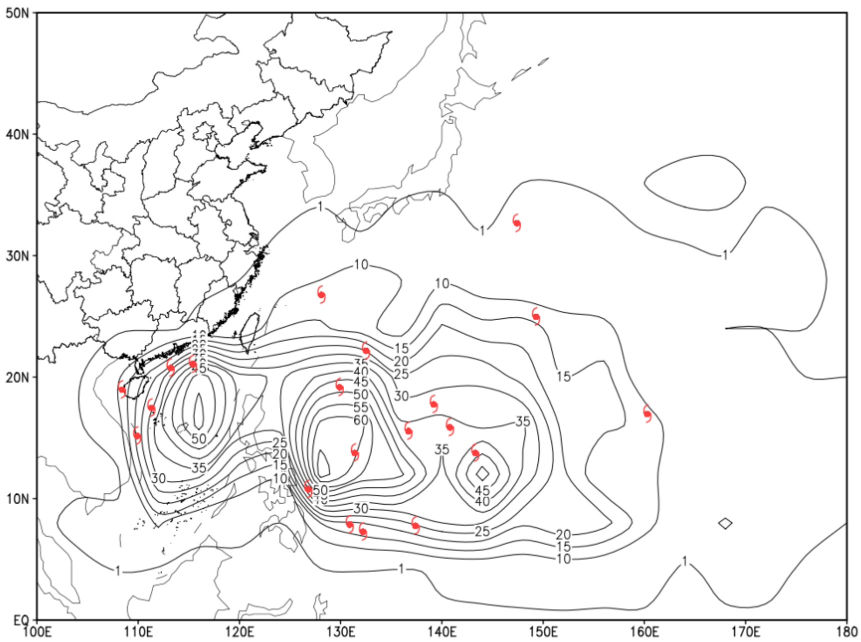

Fig. 1.3 1949-2020 NWP and SCS tropical cyclone source region density distribution (resolution: 2.5°×2.5°) and genesis location of tropical cyclones forming from 1 January to 15 November 2021

4) Fewer Landfall TCs with Weaker Intensity

Up to November 15th, 2021, 5 TCs made landfall in China. They are IN-FA, CEMPAKA, LUPIT, LIONROCK and KOMPASU. The number of making landfall in China is 1.9 less than the average, but as the same as that of the last year (2020). The mean intensity of the five landfall TCs is 29.4m/s, which is slightly weaker than the multi-year average (32.6m/s).

5) Rapid Intensification Cases with Extremely Peak Intensity

Although the 20 TCs were generally weak, three of them reached Super Typhoon grade. They are SURIGAE (2102) and CHANTHU (2114) with the peak intensity of 68m/s, and MINDULLE (2116) with the peak intensity of 60m/s. The proportion of Super Typhoon in the total this year is lower 3.2% than the average (18.2%) of the past 30 years. In the past 72 years, there were 142 TCs with peak intensity of 68m/s or above (about 2 per year on average) and 14 TCs in the past 30 years (about 1 per year on average). SURIGAE, CHANTHU and MINDULLE are all experienced rapid intensification. CHANTHU intensified from 18m/s to 58m/s from 00UTC 7 to 00UTC 8 September. The amplification in 24 hours is up to 40m/s. This has never happened in the last 30 years. However, this situation has appeared 32 times in the earlier historical record, among which the maximum increase value can reach 55m/s.

1.1.2 Precipitation of TCs Affecting China

Up to November 15, 2021, A total of 124 rivers in Zhejiang, Shanghai, Anhui, Jiangsu, Shandong, Inner Mongolia and Heilongjiang provinces were flooded by five landing typhoons. Among them, IN-FA (2106) lead the most destructive damage to the coastal and inland areas. The main characteristics of IN-FA precipitation are as follows:

1) Widely Range and Large Accumulated Amount of Rainfall

Severe Typhoon IN-FA (2106) has affected six river or lake basins in 14 provinces, namely Taihu, Yangtze, Huaihe, Yellow, Haihe and Songliao. The accumulated amount of rainfall exceeds 150mm in 24 cities in Zhejiang, Shanghai, Jiangsu, Anhui and Shandong provinces, among them 15 cities over 200mm. The heaviest rainfall with 1010mm occurred in Dongling Town, Huzhou City, Zhejiang Province. The maximum daily rainfall amount was observed 506mm in Xiajialing Town, Ningbo city, Zhejiang Province. The total precipitation amount of IN-FA is about 127.4 billion cubic meters, ranking the fifth of that landing typhoon in China since 1949.

2) Exceeding Warning Floods and High Level River Network

In Zhejiang, Jiangsu, Shanghai, Anhui, Shandong, Inner Mongolia and Heilongjiang provinces, 48 rivers experienced floods when severe typhoon IN-FA (2106) made landfall. The first flood of Taihu Lake and the third flood of Nenjiang River occurred. Among them, the highest water level of Taihu Lake is 4.20 meters (0.40 meters above the warning level). During the impact of IN-FA, the water level of the river around Taihu Lake has exceeded the warning level. 10 stations in Zhejiang, Hangzhou and Shanghai broke the records. The water level of Hongze Lake, Luoma Lake and Nansihu lake in Huaihe River basin exceeded the flood limits by 0.20 ~ 0.51 meters, and the water level of 27 stations in Lixia River area in Jiangsu Province exceeded the warning levels.

3) Gale Winds, Rainfall, Tide and Floods Superimposed Effect

During the impact period of Severe Typhoon IN-FA (2106), the water level of 14 small and medium-sized rivers, including Puyang River and Caoe River, tributaries of Qiantang River, Yaojiang river and Gulin River, tributaries of Yongjiang River, and Baiquan Main River along northeastern coast of Zhejiang Province, have exceeded over guaranteed water level. In the coastal areas of Fujian, Zhejiang, Shanghai and Jiangsu, 42 tide stations exceed 0.02 to 1.24 meters, and 5 stations exceed 0.18 to 0.67 meters of the warning level. In Ningbo and Zhenhai of Zhejiang, Zhujing, Maogang, Mizidu, Shagang and Songpu Bridge of Shanghai, 11 stations exceed the highest historical tide records.

1.1.3 TCs Affecting China

1) Severe Typhoon IN-FA (2106)

IN-FA formed over the NWP at 1800UTC on 7 July, 2021. It intensified into a severe tropical storm at 0000UTC on 19 July, then upgrade to typhoon at 0600UTC on 20th. At 0300UTC on 21 July, IN-FA developed into a severe typhoon. Around 0430UTC on 25th, it made landfall over the coastal area of Zhoushan, Zhejiang Province with the intensity of 38m/s (typhoon). Across Hangzhou Bay, IN-FA made its second landfall at 0150UTC on 26 July on the coast area of Pinghu, Zhejiang Province with the intensity of 28m/s (severe tropical storm). Then it weakened into a tropical depression in Anhui Province at 1900UTC on 28th, and moved into the Bohai Sea from Huanghua of Hebei Province in the morning of 30 July and then transitioned to an extra-tropical cyclone in the evening of 30 July.

Under the impact of IN-FA, from 22 July to 1 August, 7 provinces which are Zhejiang, Jiangsu, Anhui, Shandong, Hebei, Henan, Liaoning and 4 cities which are Shanghai, Tianjin, Shangqiu and Zhoukou experienced 100 to 250mm accumulated amount of rainfalls. There are 300 to 600mm amount of rainfall in northern and eastern part of Zhejiang province, Shanghai city, southeastern Anhui province and Jiangsu province, and 700 to 900mm in the northern part of Zhejiang province. The maximum accumulated amount of rainfall (1034.3mm) is captured at Dingjiafan station, located in Yuyao town of Ningbo city. Meanwhile, the rainfall in central and northern Taiwan was 200 ~ 400mm, exceeding 500 mm in local.

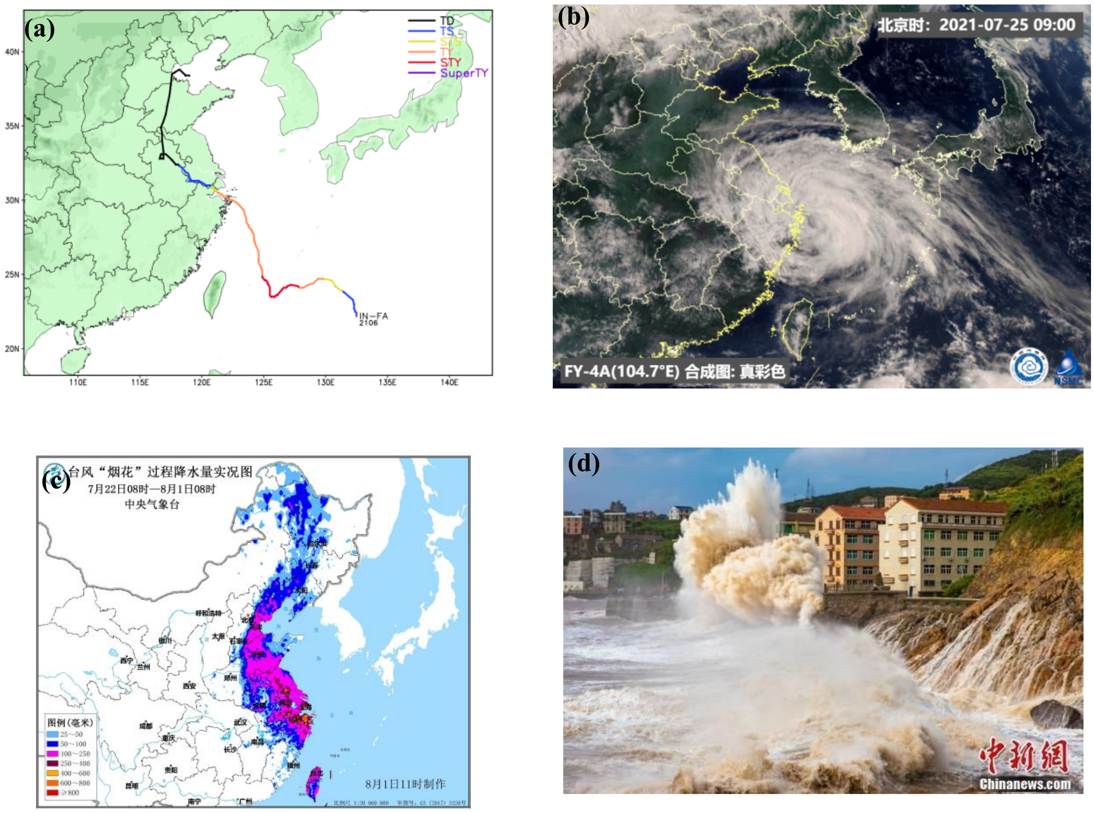

Fig. 1.4 (a) Track, (b) Satellite Image, (c) Accumulated Precipitation, and (d) Hazards of Severe Typhoon IN-FA

2) Tropical Storm CEMPAKA (2107)

Tropical Storm CEMPAKA formed over the northern part of the SCS at 0600UTC on 18 July, intensified into a tropical storm at 1800UTC at the same day. CEMPAKA strengthened into a severe tropical storm at 0900UTC on 19th, and then developed into a typhoon six hour later at 1500UTC. CEMPAKA made landfall over the coastal area of JiangCheng District, Yangjiang city, Guangdong Province around 14:50UTC on 20 July with the intensity of 33m/s (typhoon). After passing over the western part of Guangdong Province, CEMPAKA moved into southern part of Guangxi

Province and moved westward. CEMPAKA continued to weaken after moving into the Beibu Gulf on the morning of July 22, and it was ceased to be registered at 1200UTC on 24th.

Under the influence of CEMPAKA, from 19th to 23rd July, the coastal area of Guangdong Province and northern part of Hainan Island experienced gusts of scales 7 to 8, gusts of scales 9 to 10 occurred at some individual islands, Nanpeng Island of Yangjiang, Guangdong Province experienced gusts up to 48.7m/s (15 scale). Over central and southern parts of Guangxi province, coastal area of central eastern part of Guangdong province, southeastern part of Fujian province and northeastern part of Hainan Island, the accumulated amount of precipitation attained 50 to150mm, which up to 180 to 344mm over Yangjiang and Maoming, Guangdong Province and Beihai, Guangxi Province.

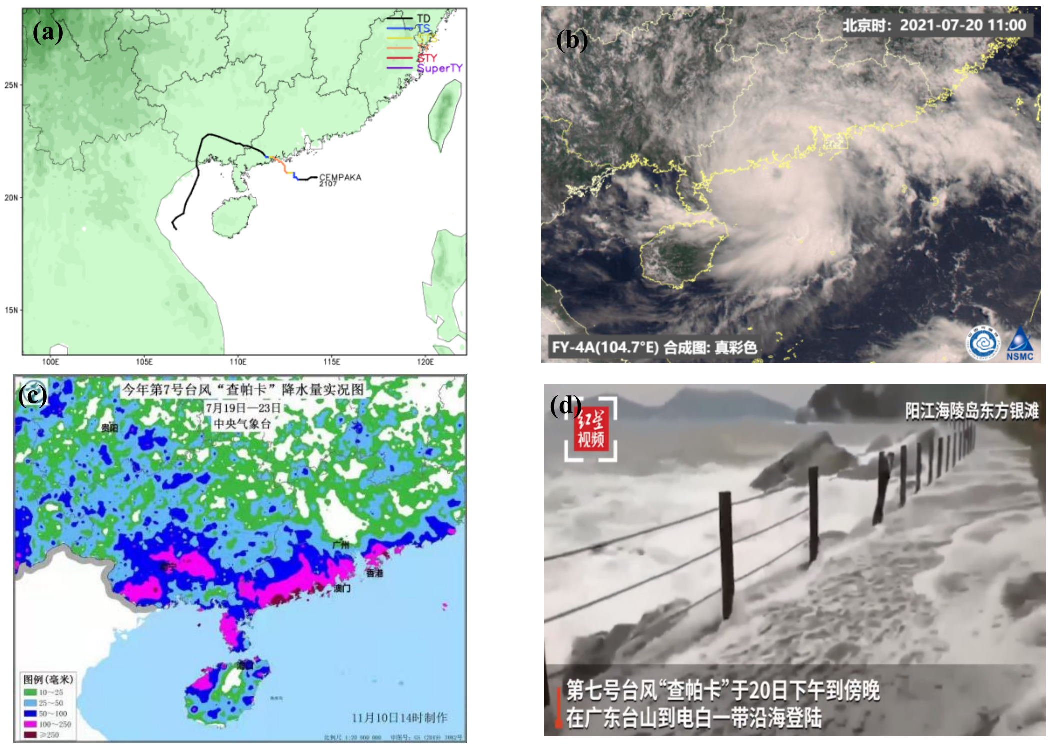

Fig. 1.5 (a) Track, (b) Satellite Image, (c) Accumulated Precipitation, and (d) Hazards of Tropical Storm CEMPAKA

3) Tropical Storm LUPIT (2109)

Tropical Storm LUPIT formed over the offshore east of Leizhou Peninsula at 0900UTC on 2 August, strengthened into a tropical storm at 0000UTC on 4th and moved northeastward. LUPIT made first landfall over the coastal area of Nan'ao County, Shantou city, Guangzhou Province with the intensity of 23m/s (tropical storm) and moved toward northeast along the coastal of Guangdong and Fujian province, and then made its second landfall over the coastal area of Dongshan County, Zhangzhou city, Fujian Province with the intensity of 18m/s (tropical storm). After making landfall, LUPIT weakened to a tropical depression and intensified once again after moved into Taiwan Strait. Passing over northern part of Taiwan Island, LUPIT strengthened slightly, and made its third landfall on the coastal area of Kagoshima, Japan at 1200UTC on 8th with intensity of 20m/s (tropical storm). LUPIT have transited to an extratropical cyclone gradually since landfall, and it was ceased to be registered at 0600UTC on 9th.

Under the combined effects of LUPIT and monsoon, from the evening of 4 to 7 August, including central southern part of Hunan, central southern part of Jiangxi, eastern and southern parts of Zhejiang, Fujian, Guangdong, eastern part of Guangxi, northern part of Hainan and Taiwan Island, eight provinces experienced heavy rainfall. Some coastal areas of southeastern of Zhejiang, eastern part of Fujian, Guangdong, southeastern part of

Guangxi and southern part of Taiwan Island experienced heavy rainfall or torrential rain locally. The accumulated precipitation amount of the regions mentioned above is generally 30-80 mm, 150 to 250mm in some areas and with local rainfall exceeding 350 mm. Meanwhile, some areas experienced strong convective weather such as short-term heavy rain and locally thunderstorm, the maximum hourly precipitation amount is 30 to 60mm, with local rainfall exceeding 80mm.

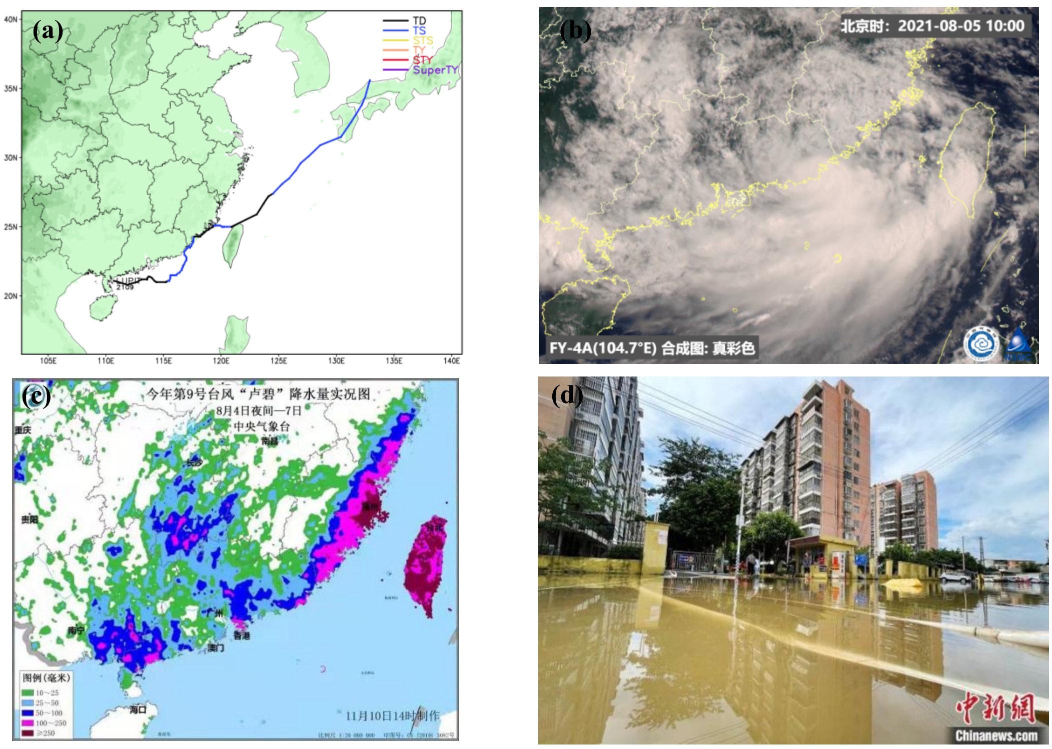

Fig. 1.6 (a) Track, (b) Satellite Image, (c) Accumulated Precipitation, and (d) Hazards of Tropical Storm LUPIT

4) Tropical Storm LIONROCK (2117)

Tropical Storm LIONROCK formed over the central SCS at 0000UTC on 6 October and upgraded to tropical storm at 2100UTC on the next day before moving northward. LIONROCK moved north-northwest with steady intensity, it made landfall over Qionghai of Hainan around 1450UTC with the intensity of 20 m/s (TS, 990hPa), and moved further northwestward. After passing over north-central Hainan Island and went into Beibu Gulf at 1500UTC on 9th, LIONROCK made its second landfall at 0820UTC on 10th in Northern Vietnam (TS, 18 m/s, 990hPa), and was finally dissipated at 1200UTC 10th in Vietnam.

Under the impact of LIONROCK, the accumulated rainfall from 8th to 11th is 200-400mm in central and western Guangdong, southern Guangxi, and central and northern Hainan, with locally 450-557mm in Lingao, Changjiang and Baisha of Hainan, Zhongshan and Zhuhai of Guangdong, Fangchenggang of Guangxi. Meanwhile, gusts over coastland of South China reached scales 7 to 9 and scales 10 to 11 locally along the central and western coast near Guangdong, northern Hainan Island and eastern Guangxi.

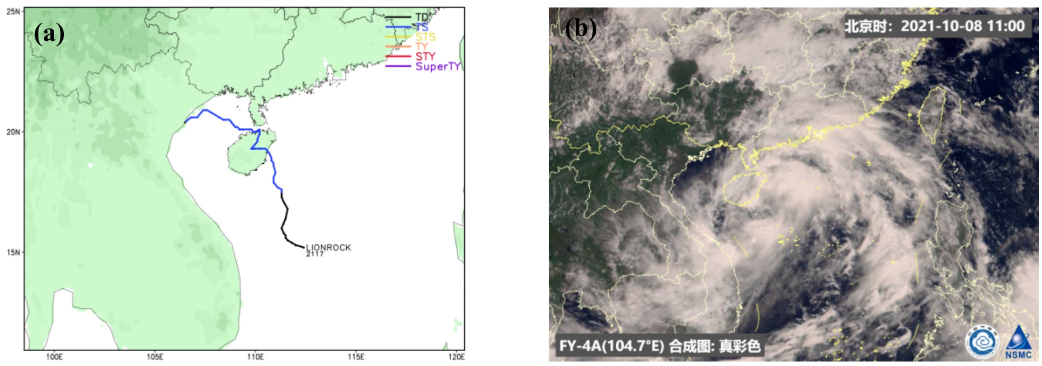

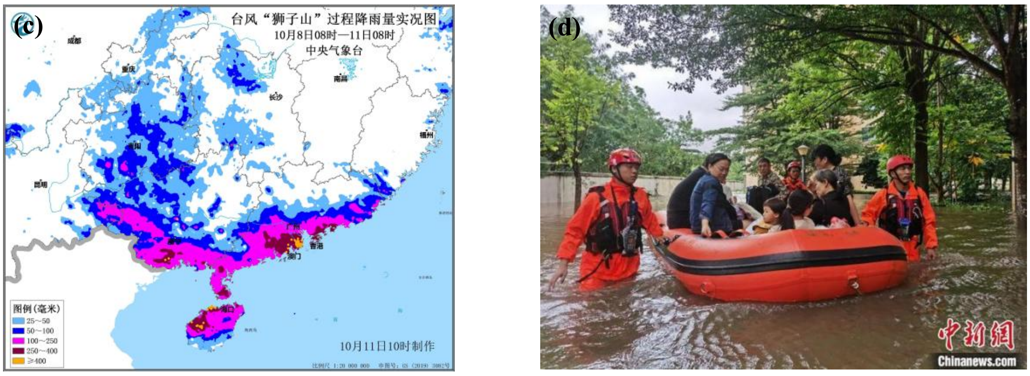

Fig. 1.7 (a) Track, (b) Satellite Image, (c) Accumulated Precipitation, and (d) Hazards of Tropical Strom LIONROCK

5) Typhoon KOMPASU (2118)

Typhoon KOMPASU (2118) formed as a tropical low over the Ocean to the east of the Philippines at 1800UTC on 7 October, then it gradually intensified to a tropical storm at 0900UTC on 8th and moved westward. After passing over the northern Luzon Island of Philippines, it intensified to a severe tropical storm at 1500UTC on 11th and to a typhoon at 2100UTC in the next day. KOMPASU made its landfall over Qionghai of Hainan Island with the intensity of 33m/s (typhoon). After the landfall, it continued moving westward and weakened. After crossing Hainan Island and Beibu Gulf, it made second landfall over the coastal area of northern Vietnam around 1130UTC on 14th (14 m/s, TD), getting dissipated immediately. It was ended to be registered at 1200UTC in Vietnam.

During 11th to 14th, gusts over coastland of Zhejiang and Fujian, Guangdong, Guangxi, Hainan Island, Taiwan Island, Dongsha Islands, Xisha Islands reached scales 8 to 10; 11 (28 m/s) over North Reef of Yongxing Island, 15 (48.6 m/s) over Wenchang Qizhou Islands of Hainan.

KOMPASU landed over Qionghai of Hainan closely followed LIONROCK (2117). The rainfall caused by these two TCs were highly overlapped over parts of Guangdong and Hainan. Accumulated rainfalls ranged 100-250 mm over coastal area of Guangdong, southern Guangxi, south-central Hainan and Taiwan and 250-320 mm in eastern Taiwan, peaked 328 mm locally over Qionzhong of Hainan. In addition, accumulated rainfalls 100-300 mm happened over eastern Zhejiang, northeastern and central Fujian, with locally 400-490 mm over Wenzhou and Taizhou of Zhejiang and Ningde of Fujian.

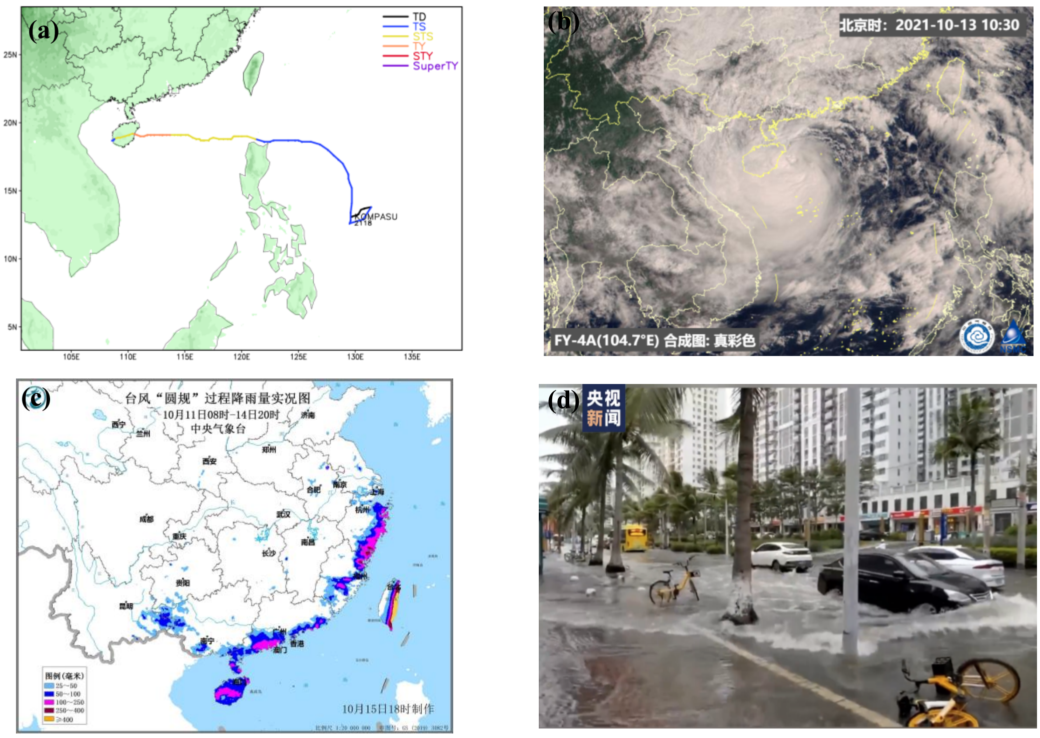

Fig. 1.8 (a) Track, (b) Satellite Image, (c) Accumulated Precipitation, and (d) Hazards of Typhoon KOMPASU

1.1.4 Climatic Prediction of TCs

Beijing Climate Center (BCC) issues seasonal forecast of the NWP tropical cyclone genesis and landfall numbers, prevailing moving tracks and intensity in March and May each year based on statistical approaches and hybrid statistical-dynamical models.

1) Annual Prediction of TCs

The tropical cyclone activity in 2021 over the NWP and the SCS will be above normal, with number of genesis is 27-29 and 8-10 landfalls. The overall intensity of tropical cyclones is moderate to weak. The prevailing moving track is northwestward, with potential of northward moving TCs which might impact eastern South China and East China. The date of first tropical cyclone making landfall will be earlier than climatology (28 June), and the last later than climatology (6 October).

2) Prediction of TCs during Boreal Summer

The amount of TCs generated during boreal summer of 2021 over the NWP and the SCS will be equal to climatological mean (11), among which 4 to 5 TCs will make landfall over China. The intensity of TCs is moderate or weak. The prevailing track is westward or northwestward, which might greatly impact South China and East China.

The observed number of TCs genesis during summer is 9, with 4 made landfall over China, less than climatological mean. There exists a deviation of predicted TCs genesis frequency. However, the predicted intensity and prevailing TCs track are in accordance with observational results, including the possibility of northward moving TCs.

1.2 Socio-Economic Assessment

By November 15th, 2021, 7 TCs affected China, 5 of which made landfalls at the mainland. According to preliminary statistics, TCs in this year have affected population of 6.44 million people in 13 provinces (autonomous region), with 4 deaths, evacuations of 1.61 million people and relocated population of 1.98 million people, about 800 collapsed and over 9,400 damaged houses, and affected crops of 441,200 hectares and destroyed crops of 44,500 hectares.

On July 20th, CEMPAKA (2107) made landfall in Guangdong. It was the first TC that hit China this year, whose landfall was more than one month later than the usual date (June 17th). On 25 and 26 July, typhoon IN-FA (2016) made landfall at Zhoushan and Pinghu in Zhejiang successively, and it became the first typhoon that hit Zhejiang twice since 1949. After its landfall, IN-FA moved northward and demonstrated features of strong wind, heavy rainfall, long duration, and wide-ranged impact. IN-FA totally damaged 8 provinces (autonomous region) and caused 4.82 million people affected, 1.14 million people evacuated, 1.43 million people relocated, and over 8,300 rooms damaged, which made it the most destructive TC to China in this year.

Table 1 Statistics of TCs landfalls and losses in China.

TC Name and Number	Landing date, intensity, location	Affected province	Affected population (10^4 people)	Dead toll (Person)	Emergency evacuated population (10^4 people)
IN-FA (2106)	0430 UTC, 25 Jul. / TY Zhoushan, Zhejian 0150 UTC, 26 Jul. /STS Pinghu, Zhejian	Hebei, Inner Mongolia, Liaoning, Shanghai, Zhejiang, Anhui, Shandong	482.0		114.1
CEMPAKA (2107)	1350 UTC, 20 Jul. / TY Yangjiang, Guangdong	Guangdong, Guangxi, Hainan	6.3		1.1
LUPIT (2109)	0300 UTC, 5 Aug. / TS Shantou, Guangdong 0850 UTC, 5 Aug. / TS Zhanghou, Fujian	Fujian	7.4	1	3.2
CHANTHU (2114)		Shanghai, Jiangsu, Zhejiang	85.1		25.6
LIONROCK (2117)	1450 UTC, 8 Oct. / TS Qionghai, Hainan	Guangdong, Guangxi, Hainan	34.7	1	7.4
KOMPASU (2118)	0740 UTC, 13 Oct. / TY Qionghai， Hainan	Fujian, Guangdong, Guangxi, Hainan, Yunnan	28.5	2	10.0
Total			644	4	161.4

1.3 Regional Cooperation Assessment

1.3.1 International Training Course on Typhoon Operations of CMA

From 9th to 11th in December 2020, CMATC joined National Meteorological Center completed 2020 Typhoon Committee member forecaster operational training course, namely The 5th International Training Course on Typhoon Operations of China Meteorological Administration, which is intended to enable trainees to learn TC monitoring analysis and forecast technology, strengthen the collection of meteorological satellite data and the application of ensemble forecast products, promote the operational communication between members of the Typhoon Committee. The training course has enrolled 44 international trainees from 19 countries and regions.

1.3.2 Progress of Tropical Cyclone Research and Review in 2021

Up to November, the third issue of 2021 TCRR (Tropical Cyclone Research and Review) has been published. This year TCRR has published a special issue on typhoon-related flood and disaster risk reduction. At present TCRR is cooperating with the globally familiar publisher, Elsevier BV through KeAi Communications Co., Ltd. to enhance the journal's citation frequency. And the Scholar One Manuscripts submission and peer-review system of Clarivate Analytics are also employed. In May 2021, the editors participated in the nineteenth National Workshop on Tropical

Cyclone held in Qingdao to publicize TCRR. Posters and flyers were prepared for this exhibition.

Currently, TCRR has been included in three full-text databases, including Science Direct, DOAJ, and CNKI. As a result, all of the published papers are easily and freely available from these full-text databases. Based on the available statistic data, the readers spread over 126 countries and regions. In the past two years, the full-text downloads via Science Direct alone have exceeded 80,000 times a year. 60 articles published between 2018 and 2020 have been cited 223 times. TCRR has also been indexed by the Emerging Sources Citation Index (ESCI), which is same as SCI, owned by the Clarivate Analytics.

II. Summary of Progress in Priorities supporting Key Research Areas

2.1 Application of Machine Learning in the Technique of Typhoon Vortex Detection

Meteorological satellite is the most effective and primary monitoring tool for typhoon. FY satellite can provide the satellite cloud images with high temporal and spatial resolution in real time. In order to better use the satellite cloud images to monitor the typhoon definitely, combining with Artificial Intelligence (AI), which has developed rapidly in recent years, the National Meteorological Center (NMC) has explored the application of machine learning in typhoon vortex detection.

Based on the satellite images and the typhoon best track data of China Meteorological Administration, the classical target detection SSD model with fast running speed and high recognition accuracy is used as the basic model of typhoon vortex detection. Based on the characteristics of typhoon vortex, especially for detection of the weak vortex, the SSD model is improved and optimized, and then an iterative SSD target detection model is given out. Finally, the intelligent typhoon vortex recognition technique is established by training and testing of the model. The technique can intelligently detect all the typhoon vortex of the satellite infrared image and all can define the location of the vortex center. The application of machine learning in typhoon vortex detection is a new exploration. This technology has excellent detection ability for typhoon vortex. Results show that the correct recognition rate of typhoon with intensity below severe tropical storm (STS) level is 40-80%, the correct rate of typhoon with STS level and above is more than 90%, especially the recognition rate of typhoon level and above is very close to 100%. This technology can support the real-time and precise monitoring of typhoon by using high temporal and spatial resolution satellite data in the future.

Priority Areas Addressed:

Meteorology

- Enhance the capacity to monitor and forecast typhoon activities particularly in genesis, intensity and structure change.
- Develop and enhance typhoon analysis and forecast technique from short- to long-term.

Contact Information:

Member: China

Name of contact for this item: Qian Qifeng

Telephone: +86-010-58993910

Email: qianqf@cma.gov.cn

2.2 Advances in Numerical Modeling of TCs

2.2.1 Center for Earth System Modeling and Prediction of CMA Established

The Center for Earth System Modeling and Prediction of CMA has been established in October 2021. The global and regional tropical cyclone (TC) prediction systems GRAPES_GFS and GRAPES_TYM were renamed to CMA-GFS and CMA-TYM, respectively. The main progresses are as follows:

1) Operational Upgrade for Regional TC Prediction Model CMA-TYM

CMA-TYM was operational upgraded in May 2021, the main promotions including: 1) the basic version of model was promoted from V4.4 to V5.0; 2) the parameter of surface layer roughness was optimized; 3) the parameter of local diffusion coefficient related with vertical diffusion was changed; 4) the static data and surface process of model was upgraded; 5) scale-aware cumulus parameterization was improved; 6) cloud analysis was applied; 7) the predictions for TCs over the Northern Indian Ocean has been realized through the establishment of TC forecast module for this basin.

The hindcast results for 2018-2020 show that the promotions for CMA-TYM V3.2 could efficiently reduce the errors for TC track and intensity (Fig. 2.2) and significantly improve the prediction skills for precipitation.

2）Operational Upgrade for Global Prediction Model CMA-GFS

CMA-GFS has been operational upgraded twice during 2021. In June 2021, the promotion for the model physics was completed and the version of CMA-GFS was upgraded from V3.0 to V3.1. The main improvements contain land and cumulus convection processes. In September 2021, the version of CMA-GFS was upgraded to V3.2 and realized the predictions for TCs over global basins, the main changes including:1) processing for TC data in global ocean was established; 2) the hourly assimilation for TC data was applied in the initialization of TC; 3) post-processing for global TC was built and the related products was developed; 4) the data of track and intensity have been disseminated through CMA CAST. The scheme for hourly assimilation of TC center pressure used in the global TC predictions was showed in Fig. 2.3.

3) Real-time Running of Regional Ocean-atmosphere Coupling Model

The real-time running of regional ocean-atmosphere coupling model CMA-TYM-HYCOM has been implemented since May 2021.

2.2.2 Dynamical-Statistical hybrid Seasonal Prediction of TC Track Density over Western North Pacific

Compared with total account of basin-wide TC genesis, the prevailing tracks of TC activity and its potential of landfalling is more important for disaster prevention. Despite its relatively lower predictability, a statistical-dynamical hybrid prediction model was developed based on the physical mechanisms between the western North Pacific (NWP) TC activity and related large-scale environmental backgrounds from July to September. The leading modes of spatial-temporal variation of the NWP TC tracks density were extracted by using empirical orthogonal function (EOF). The interannual variation of leading EOF modes of NWP TC track density was predicted using multiple linear regressions (MLR) method based on predictors selected by correlation analysis of both observational and Beijing Climate Center climate system model version 1.1 (BCC_CSM1.1) hindcast data. The predicted spatial distribution of NWP TC tracks density was obtained through weighted composite of forecasting EOF modes according to its explained variance respectively. Results of one-year-out cross validation indicate that forecast model well captures the interannual variation of NWP TC prevailing moving tracks, especially in the South China Sea (SCS) and southeastern quadrant of NWP. The prediction skills enhanced with forecast leading time decreasing, and anomaly correlation coefficient (ACC) of the northern SCS and southeast quadrant of NWP reaches 0.6 for the period of 1991-2020 with one-month leading time (Fig. 2.4). Forecast assessments based on different ENSO phases indicate that source of predictability of NWP TC tracks was mainly originated from ENSO events, especially strong El Niño events.

2.2.3 The Operational Running of TRANSV1.0

The Typhoon Rapid Refresh Analysis and Nowcasting System (TRANSv1.0) is jointly developed by the Chinese Academy of Meteorological Sciences, National Meteorological Centre, Guangdong Institute of Tropical and Marine Meteorology and Nanjing University. Since the quasi-operational running of TRANSv1.0 on 6 August, 2020, the track and intensity of landfall TCs are well captured, it also provides accurate predictions of heavy-hard rain and torrential rainfall. CMA officially approved the operation of the TRANSv1.0 on 15 January, 2021. Up to 12 November, 2021, TRANSv1.0 has carried out real-time forecasts for the all 5 landfall TCs and one TC (CHANTHU) which affected coastal areas of China in 2021. The forecast time could satisfy the needs of current operational forecast, and the products have been widely used in the national TC forecast consultation (Fig. 2.5).

TRANSv1.0 integrates the cycling Kalman-filter assimilation technique, which would employ hourly assimilation when a TC observed by the coastal radar network, and provide a 12-hour ranged forecast product. The radar radial wind Evenly-Spaced Thinning Method (ESTM) adopted by the system can effectively improve the utilization of TC inner-core observations, which can enhance the accuracy of the predictions about TC structure and extremely precipitation generated by TC. The real-time operation of the TRANSv1.0 effectively improves the application of radar observation in the real-time TC numerical modeling.

2.2.4 Upgrade for CMA-TRAMS

To improve the performance of China Meteorological Administration Tropical Region Atmospheric Modeling for South China Sea (CMA-TRAMS), some model schemes have been improved, including the 3D referenced atmosphere scheme and semi-implicit semi-Lagrangian (SISL) method in dynamical core, as well as the physical parameterization schemes and cloud analysis technique. In addition, some new model techniques have been developed. For example, a time-varying referenced atmosphere scheme and a computational method improving the low-level advection calculation were developed.

The performance of CMA-TRAMS in 2021 is stable, and till November, 20 TCs have been successfully forecasted. In terms of predictions of TC genesis, CMA-TRAMS have predicted the genesis of LIONROCK and KOMPASU 144-hour earlier. From the aspect of TC track and intensity forecast, the 24h, 48h and 72h predicted track errors of

IN-FA, which made landfall in China, were 42.5km, 73.5km and 161.1km respectively, and the 24h, 48h and 72h forecasted intensity errors were 3.95hPa, 9.63hPa and 11.64hPa respectively. The 24h, 48h and 72h forecasted track errors of KOMPASU, which significantly affected the South China Coast, were 138.48km, 145.15km and 166.95km, and the 24h, 48h and 72h intensity errors were 5.95hPa, 7.52hPa and 5.68hPa, respectively. In addition, the persistent heavy rainfall in Zhengzhou, Henan brought by the severe Typhoon IN-FA, was also accurately predicted by CMA-TRAMS.

Priority Areas Addressed:

Meteorology

- Enhance the capacity to monitor and forecast typhoon activities particularly in genesis, intensity and structure change.
- Develop and enhance typhoon analysis and forecast technique from short- to long-term.

Contact Information:

Member: China

Name of contact for this item: Ma Suhong

Telephone: +86-010-58993910

Email: suhong0228@hotmail.com,

Name of contact for this item: Yin Yizhou

Telephone: +86- 010-58990142

Email: yinyizhou@cma.gov.cn

Name of contact for this item: Wang Hui

Telephone: +86-010-58994270

Email: huiwang@cma.gov.cn

Name of contact for this item: Li Mengjie

Telephone: +86-020-39456473

Email: limj@gd121.cn

2.3 Tropical Cyclone Observation Experiment

2.3.1 Field Detection Experiment of Severe Typhoon IN-FA

The field detection experiment was successfully carried out near the center of IN-FA in Zhoushan, Zhejiang Province from 23 to 26 July, 2021 (Fig. 2.6-a). GPS sounding, boundary layer wind profile, laser raindrop spectrum and automatic observed weather station were employed during the period that IN-FA landfalling, passing and slowly moving. At the same time, ozone sounding balloons were successfully released before, after and when IN-FA making landfall (Fig. 2.6-b), which is the third ozone detection experiment of the typhoon circulation in China following LEKIMA in 2019 and NANGKA in 2020.

Figure 2.7 shows that the variations of ozone in the lower troposphere changed significantly before and after the landfall of IN-FA. The concentration of ozone decreased when the typhoon approaching, and it dropped to the lowest when IN-FA making landfall, then it increased after the typhoon passed. However, when the altitude higher than 18km, there is basically no change of the ozone concentration, indicating that the convection of typhoon does not reach this height.

2.3.2 Filed Experiment of Tropical Storm LIONROCK in 2021

According to the research plan of “Key Technology Research and Demonstration for Comprehensive Monitoring and Early Warning of

Typhoon and Gale Disaster Risk" of Guangdong Province's key field research and development project, the field experiment of the tropical storm LIONROCK was carried out at the Marine Meteorological Scientific Experiment Base in Xuwen, Zhanjiang, Guangdong Province, and the different levels of wind data were obtained through the gradient towers. LIONROCK (2117) formed in the south of the Xisha Islands in the South China Sea at 0000UTC on 6 October, 2021, and made landfall at Qionghai, Hainan at 1450UTC on 8 October (20m/s). Then it moved into the Qiongzhou Strait. At about 0800UTC on 9 October, the tropical storm was the closest to Xuwen Marine Meteorological Scientific Experiment Base. The observation data of the tower in Figure 2.8 shows that the wind speed decreasing when the lowest pressure occurred, indicating that the center of the storm passed over the observation point.

Priority Areas Addressed:

Meteorology

- Enhance the capacity to monitor and forecast typhoon activities particularly in genesis, intensity and structure change.
- Develop and enhance typhoon analysis and forecast technique from short- to long-term.

Contact Information:

Member: China

Name of contact for this item: Yu Zifeng

Telephone: +86-021-54896105

Email: yuzf@typhoon.org.cn

Name of contact for this item: Li Mengjie

Telephone: +86-020-39456473

Email: limj@gd121.cn

2.4 CMA Enhances Forecast Reviews over Significant TC Events

In order to improve the understanding of evolution processes and mechanisms for severe weather, CMA strengthens the forecast-review activities, focusing on the forecast difficulties and science issues related with weather events, including severe disaster weather, high-impact weather, or major weather events of high social concerns. In case of large forecast deviation for significant weather, forecasters will also carry out post-analysis, trying to find the contributed reasons. Forecast-review activities are conducted jointly by national centers and local Met. Offices.

For the TCs which made landfall or highly impacted upon China, typhoon IN-FA (Fig. 2.9) and CHANTHU (Fig. 2.10) are selected as the major cases for forecast reviews, with the purpose of summarizing the TCs characteristics, forecast difficulties, numerical weather prediction performance, and involved scientific problems, and trying to answer the ultimate question "whether or not we could do better forecast next time?". In all, forecast reviews have provided a good platform and opportunity for forecasters, especially for young forecasters to gain more forecast experiences and improve their capabilities to face future forecast challenges.

Priority Areas Addressed:

Meteorology

•Enhance the capacity to monitor and forecast typhoon activities particularly in genesis, intensity and structure change.

•Develop and enhance typhoon analysis and forecast technique from short- to long-term.

•Enhance and provide typhoon forecast guidance based on NWP including ensembles and weather radar related products, such as QPF/QPE.

Contact Information:

Name of contact for this item: Dong Lin

Telephone: +86-010-68400133

Email: donglin@cma.gov.cn

Name of contact for this item: Qian Chuanhai

Telephone: +86-010-68409321

Email: chqian@cma.gov.cn

2.5 Successfully Launched Fengyun-4B and Fengyun-3E satellites

FY-4B satellite was successfully launched at the Xichang Satellite Launch Center on June 3, 2021. It is the first operational satellite of the new generation of geostationary orbit meteorological satellites. FY-4B and the FY-4A satellite which successfully launched on 11 December 2016, constitute a geostationary orbit meteorological satellite network system, which realizes the high-frequency monitoring of atmosphere and clouds, obtains the vertical information of the clear sky and thin cloud regions and generates various physical parameters and quantitative products. The fast imager, radiation imager data and products of the FY-4B provide trial application service for three typhoons (IN-FA (2106), CEMPAKA (2107) and NEPARTAK (2108)) and the process of heavy rain in Henan Province. The FY-4B fast imager 1 minute 250-meter resolution data and animation were applied to monitor the development of small-scale convection in the core area of the typhoon and the interaction of the three typhoons to obtain detailed observations of continuous evolution. The water vapor transportation and distribution, development and movement of convective clouds over Henan during the precipitation process are also real-time monitored by FY-4B satellite cloud image animation.

FY-3E satellite was successfully launched at the Jiuquan Satellite Launch Center on 5 July, 2021. It is the fifth satellite of the second-generation polar-orbiting meteorological satellite and the first civil early-morning orbital meteorological satellite. FY-3E satellite is networked with the FY-3C and FY-3D satellites in orbit, which can provide a global observation per 6-hour for numerical weather prediction, effectively improving the accuracy and timeliness of global numerical weather prediction. Main instruments carried on FY-3E satellites include microwave temperature sounder, microwave humidity sounder, hyper-spectral infrared atmospheric sounder and so on. FY-3E can realize the monitoring of three-dimensional atmosphere, oceanic wind field, and nighttime visible and other elements, effectively enhance the monitoring and analysis of weather and climate. The microwave temperature and humidity profile obtained by the fusion and inversion of the microwave temperature and humidity sounder can penetrate cloud-rain and provide the three-dimensional thermal structure of typhoons. FY-3E wind, thermal structure and total precipitation observation products provided effective information for typhoon (CHANTHU (2114), KOMPASU (2118)) analysis.

Priority Areas Addressed:

Meteorology

- Enhance the capacity to monitor and forecast typhoon activities particularly in genesis, intensity and structure change.

Contact Information:

Member: China

Name of contact for this item: Wang Xin

Telephone: +86-010-68407927

Email: xinwang@cma.gov.cn

2.6 Advances in Tropical Cyclone Scientific Research

2.6.1 Identifying the Development of Tropical Depression over the South China Sea

To better understand and predict that a tropical depression develops into a tropical storm, we examine the dynamic and thermodynamic variables of 74 tropical depressions over the South China Sea, 52 of which developed into tropical storms, hereafter "developing," with the remaining being classified as "non-developing". Using the National Centers for Environmental Prediction Final (NCEP FNL) data, verified with ECMWF forecast data, we examine the dynamic and thermodynamic parameters that describe characteristics of tropical cyclones. Based on these statistical results, we propose seven criteria to determine whether a tropical depression will develop. Five had been used before, but two new criteria are also found to be helpful, which are associated with the diabatic heating rate and can used to determine whether a tropical cyclone diurnal cycle exists, 1) presence of a regular diurnal variation of the diabatic heating rate at the center; and 2) occurrence of specific peaks in the radiative-heating profile (Fig. 2.11) and whether the convection system remains intact in the center. We test all seven criteria of all tropical depression cases prior to their development or decay in 2018 and 2019. The test results show that these criteria can helpfully identify whether or not a tropical depression develops into a tropical storm in the operation with an average leading time of 36.6h before its formation.

2.6.2 The Relationship between Maximum Potential Intensity Rate of Tropical Cyclone and variation of SST

Based on TC best-track data over the western North Pacific (NWP), the OISST datasets of NOAA, and ERA-Interim reanalysis during 1982–2015, the dependence of TC MPIR (maximum potential intensification rate) on SST was analyzed. The results show that MPIR depends strongly on SST, storm intensity (the maximum sustained near-surface wind speed, Vmax), and structure (including the inner- and outer-core sizes, and outer-core wind shape), consistent with the findings for the North Atlantic TCs previously. The empirical relationship between the MPIR and SST for TCs over the NWP was constructed. The intensification rate and MPIR increasing linearly with increasing SST (Fig. 2.12). In addition, the environmental vertical wind shear (VWS) is the primary limiting factor preventing TCs from reaching their empirical MPIRs. The results suggest that even though the MPIR is largely controlled by the underlying SST but the actual IR is largely determined by both the underlying SST and the environmental factors (e.g. VWS) in both the North Atlantic and the NWP.

2.6.3 Identified Main Circulation Factors Affected the Maximum Potential Intensity Rate of Tropical Cyclone in Different Basin

Using the 6-hourly best-track tropical cyclone data and global reanalysis data for the period 1980-2017, we studied the differences about both the median and variation of tropical cyclone maximum potential intensity (MPI) as a function of sea surface temperature (SST) among basins of the North Atlantic (NA), eastern North Pacific (ENP), western North Pacific (NWP), and North Indian Ocean (NI). Results show that the median of MPI increases by 4.8, 7.7, 6.4, and 4.4m/s for each 1°C increase in SST in the NA, ENP, NWP, and NI, respectively. The MPI is the largest in the NI at SST between 27°C and 28.5°C and in the ENP at SST above 28.5°C, while is the smallest at SST below 29.5°C in the NWP. The differences of the contributions of the environmental factors to MPI were compared among basins, under same SST condition. The MPI in the ENP is largely contributed by the colder troposphere and drier boundary layer. The warmer troposphere and wetter boundary layer are responsible for the smallest MPI in the NWP. In the NA, the warmer outflow layer reduces the thermodynamic efficiency and partly offsets the positive contributions by the colder troposphere and drier boundary layer, resulting in the moderate MPI (Fig. 2.13).

2.6.4 Study on Estimation Method of the Key Parameters of Tropical Cyclone Wind Field Model in NWP Basin

The Holland B parameter is one of the key parameters of tropical cyclone (TC) wind field models. It plays a crucial role in describing the radial distribution characteristics of a TC wind field and is also widely used in TC disaster risk evaluation and other fields. In this study, a back-propagation neural network of sea surface wind field Holland B parameter ($\boldsymbol{B_s}$) is developed and verified. By using the different combinations of minimum center pressure difference, latitude, the radius of maximum wind speed, translation speed, and intensity change rate, our network is trained by the $\boldsymbol{B_s}$ values calculated from the best-track datasets of the Joint Typhoon Warning Center, and finally several models are established and validated. Results show that the performance of the neural network with only inputting central pressure difference is best. The corresponding statistical model is also established in this study and then it is compared with the neural network and existing statistical models. Results indicate that the neural network in this study can capture the nonlinear distribution phenomenon when the $\boldsymbol{B_s}$ value is large, therefore it can simulate the $\boldsymbol{B_s}$ value more accurately. it is found that the problems of the underestimation and overestimation of the two existing wind pressure models can be significantly improve when the $\boldsymbol{B_s}$ neural network is used in the wind pressure model to simulate the maximum wind speed of super typhoon (Fig. 2.14).

2.6.5 The Remote Effect of Binary Typhoon IN-FA and CEMPAKA on the "21.7" Heavy Rainfall Event

In this study, the remote effect of binary Typhoon IN-FA (2106) and CEMPAKA (2107) on the "21.7" heavy rainfall event over Henan province is investigated based on the updating CMA-SH9 system. According to the rain gauge data, there exists two heavy rainy periods during which the record-breaking extreme hourly rainfall of up to 201.9 mm occurred in Zhengzhou. In the control experiment (CTRL), the temporal-spatial distribution of precipitation in the targeted area as well as the large-scale circulation are good consistent with the observations (Fig. 2.15). By removing the relative circulation of Typhoon IN-FA (SEN1) and CEMPAKA (SEN2) in the initialization field, the water vapor flux in the targeted area is remarkably changed, leading to the decrease of accumulated precipitation as well as rainfall intensity, especially during the second rainy period. By comparing the mean vertically-integrated water vapor flux, divergences of water vapor flux and the intensity of water vapor flux from four directions during the second precipitation period, it is found that the convergence of water vapor from the east and south to is mainly water vapor source of heavy precipitation. By using the k-means algorithm, the analysis results show that more than 77% of air parcels entering the targeted area at 850hPa are transported from the easterly flow which prevails between Typhoon IN-FA and the subtropical high. A proportion of air parcels that comes from the south band increase with the increase of height, accounting for 56%, suggesting that the influence of CEMPAKA plays an important role (Fig. 2.16). Except for the moisture transportation, the interaction between the binary typhoons and their locations combing with the monsoon circulation of south and the subtropical high circulation, collaboratively impact on the occurrence of “21.7” heavy rainfall event.

2.6.6 The Gaofen-3-Retrieved Fine Ocean Surface Wind Filed of Typhoon

Gaofen-3 (GF-3) is the first Chinese space-borne multi-polarization synthetic aperture radar (SAR) installed at C-band (5.43GHz). We collected the data of VH-polarized wide ScanSAR (WSC) image and ocean surface wind speeds with 100m horizontal resolution from GF-3’s and study on the retrieved fine ocean surface wind field of Super Typhoon LEKIMA (2019). The maximum ocean surface wind speeds at 21:56:59UTC on 8 August 2019 is 38.9m/s (Fig. 2.17-a). Validating the SAR-retrieved winds with buoy-measured wind speeds, we find that the root mean square error (RMSE) is 1.86m/s and the correlation coefficients 0.92 (Fig. 2.17-b). This suggests that wind speeds retrieved from GF-3

SAR are reliable and can be used as the true value to evaluate the forecast of the models. The intensity forecast of both the European Centre for Medium-Range Weather Forecasts (ECMWF) fine grid operational forecast products and China Global/Regional Assimilation and Prediction Enhance System (GRAPES) are verified by the Gaofen-3-retrieved fine ocean surface wind. The results show that models have good performances on intensity forecast When the maximum wind of the storm is less than 24m/s) (<24m/s), but there is a larger underestimation of intensity when the storm is intensified as a severe tropical storm (>24m/s), The RMSEs are 5.24m/s for ECMWF and 5.17 m s–1 for GRAPES, with biases of 4.16m/s for ECMWF and 3.84m/s for GRAPES during Super Typhoon LEKIMA (2019).

2.6.7 The Impact of Microwave Radiance Data Assimilation on TC Track Forecast

To further strengthen the application of domestic Fengyun satellite data in the regional model, the TBB of Fengyun-3D (FY-3D) clear-sky microwave temperature sounder-2 (MWTS-2) radiances are directly assimilated in the regional mesoscale Weather Research and Forecasting (WRF) model by using the Gridpoint Statistical Interpolation (GSI) data assimilation system and then re-forecast the typhoon LEKIMA (2019). The track errors of typhoon LEKIMA decrease when the upper-air sounding data of channels 5–7of MWTS-2 is assimilated. Series experiments are conducted. One is from uses of the Advanced Microwave Sounding Unit-A (AMSU-A) radiances (EXP_AD) with those from FY-3D MWTS-2 upper-air sounding data at channels 5–7 (EXP_AMD). The results show that, the mean 24h track error can be reduced by 8.7% (~18.4km) and 30% (~58.6km) beyond 36 hours for the EXP_AD (assimilating radiances od the Advanced Microwave Sounding Unit-A (AMSU-A)) and EXP_AMD (assimilating the upper-air sounding data at channels of 5–7 FY-3D MWTS-2) respectively (Fig. 2.18), Compared with the control experiment without the assimilation of satellite radiance. The direction of simulated steering flow changes from the southwest in the EXP_AD to the southeast in the EXP_AMD, which can be a pivotal point to forecast the landfall of typhoon LEKIMA (2019) three days in advance.

Priority Areas Addressed:

Meteorology

•Enhance the capacity to monitor and forecast typhoon activities particularly in genesis, intensity and structure change.

•Develop and enhance typhoon analysis and forecast technique from short- to long-term.

Contact Information:

Member: China

Name of contact for this item: Yu Zifeng

Telephone: +86-021-54896105

Email: yuzf@typhoon.org.cn

Name of contact for this item: Wang Hui

Telephone: +86-010-58994270

Email: huiwang@cma.gov.cn

Name of contact for this item: Li Mengjie

Telephone: +86-020-39456473

Email: limj@gd121.cn

2.7 Improvement of Typhoon-related Disaster Management

2.7.1 The first National Comprehensive Survey on Natural Disaster Risks

The first National Comprehensive Survey on Natural Disaster Risks is an important survey of national conditions and capacities on disaster risk management, and a fundamental solution to improve natural disaster control and prevention. In order to figure out hidden natural hazards across the country and control capacity of natural disasters, the first national comprehensive survey on natural disaster risks will be scheduled between 2020 and 2022.

The survey will focus on six major types of disasters, including earthquake disasters, geological disasters, meteorological disasters, floods and droughts disasters, marine disasters, and forest and prairie fires. Survey missions include the following aspects: complete survey of risk components, Hazard-affected body,, historical disasters, and disaster reduction resources (capacities); survey and assessment of critical hidden hazards; construction of databases on natural disaster comprehensive risks and disaster reduction capacities by region and disaster type; assessments on single disaster risk as well as comprehensive disaster risk, and compiling a series of risk maps for natural disasters at national, provincial, and county levels; modification of risk divisions for major disaster types, and compilation of divisions for single disaster, comprehensive risk, and integrated disaster prevention and management.

2.7.2 Development of an empirical estimation model for tropical cyclone precipitation

Floods and mudslides from tropical cyclone (TC) rainstorms are among the most destructive natural hazards in China, resulting in considerable direct economic losses and large numbers of fatalities. Based on the RMS (Risk Management Solution) TC rainfall model, a number of important improvements are carried out to estimate the risk of TC rainstorm hazards in China, in which the effect of complex terrain is considered in the following three perspectives: slope, roughness and attenuation distance. In addition, extreme precipitation was redistributed by introducing spiral rain parameterization scheme Eventually, the parameterized tropical cyclone precipitation model (TCPM) is built up for long-term disaster risk assessment. The model comprehensively considers dynamic and thermodynamic efficiencies and could capture the climate characteristics of TC precipitation and probability distribution of extreme TC total precipitations over the western North Pacific (Fig. 2.19). Besides, the model is simple enough to run several hundred thousand times, which is highly portable and can be widely used in catastrophe risk assessment.

Priority Areas Addressed:

Integrated

•Enhance activities to develop impact-based forecasts and risk-based warning.

DRR

•Provide reliable statistics of mortality and direct disaster economic loss caused by typhoon-related disasters for monitoring the targets of the Typhoon Committee.

•Enhance Members' disaster reduction techniques and management strategies.

Contact Information:

Member: China

Name of contact for this item: Liu Zhe

Telephone: +86-010-52811138

Email: 76243913@qq.com

Name of contact for this item: Yu Zifeng

Telephone: +86-021-54896105

Email: yuzf@typhoon.org.cn

2.8 Tropical Cyclone Operational Skill Training of CMA

From May to June in 2021, Training Workshop on Typhoon Forecast and Early Warning was held at CMATC in Beijing. This workshop is the first special training workshop focusing on typhoon forecast and early warning in recent years, which has been widely concerned and warmly welcomed by forecasters in coastal areas. The 37 trainees were all forecasters from coastal areas or areas seriously affected by typhoon disasters.

Mixed training mode was adopted in this training workshop. In the 18-hour online training stage, the basic theoretical knowledge of typhoon was mainly consolidated; in the 2-week face-to-face training stage, the main contents of typhoon contained the research progress of typhoon theory, typhoon monitoring technology，forecast technology of typhoon track and intensity, prediction technology of typhoon precipitations and strong winds, typhoon early warning and decision-making service, typhoon forecast practice, etc. During the courses, a variety of training methods were used, such as teaching, practice, communication and discussions.

Trainees improved skills including operational capabilities of using multi-source data and abundant ideas of guiding forecast and service. A typhoon-case set was complete during this workshop.

Priority Areas Addressed:

Meteorology

•Enhance and provide typhoon forecast guidance based on NWP including ensembles and weather radar related products, such as QPE/QPF.

•Enhance, in cooperation with TRCG, training activities in accordance with Typhoon Committee forecast competency, knowledge sharing, exchange of latest development and new techniques.

Contact Information:

Member: China

Name of contact for this item: Zhang Xin

Telephone: +86-010-68405753

Email: xin09chn@sina.com

Annexes

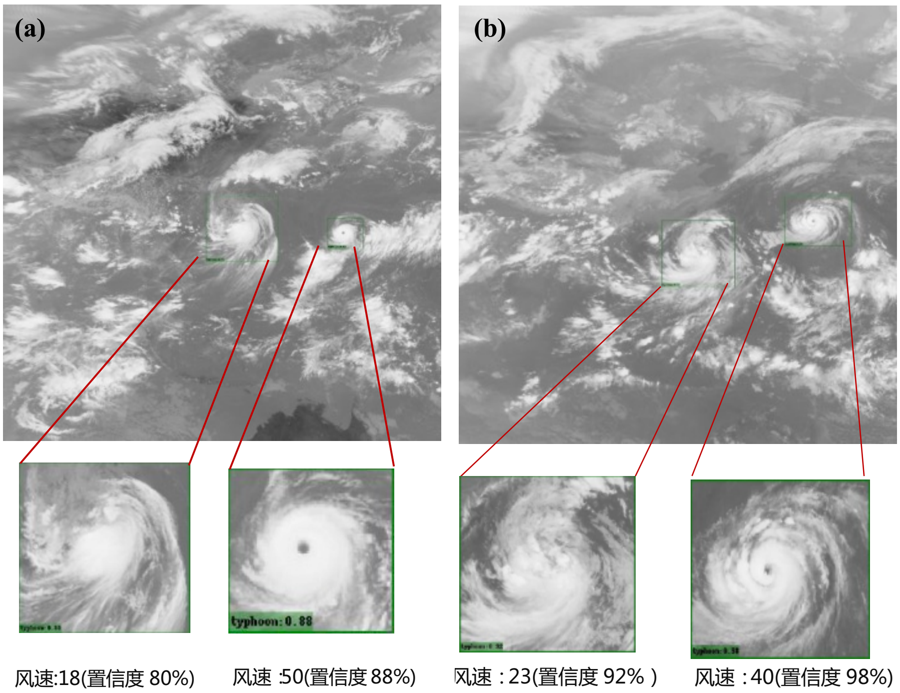

Fig.2.1 The cases of typhoon vortex detection with different intensity: (a) two vortexes with intensity 18m/s and 50m/s (b) two vortexes with intensity 23m/s and 40m/s

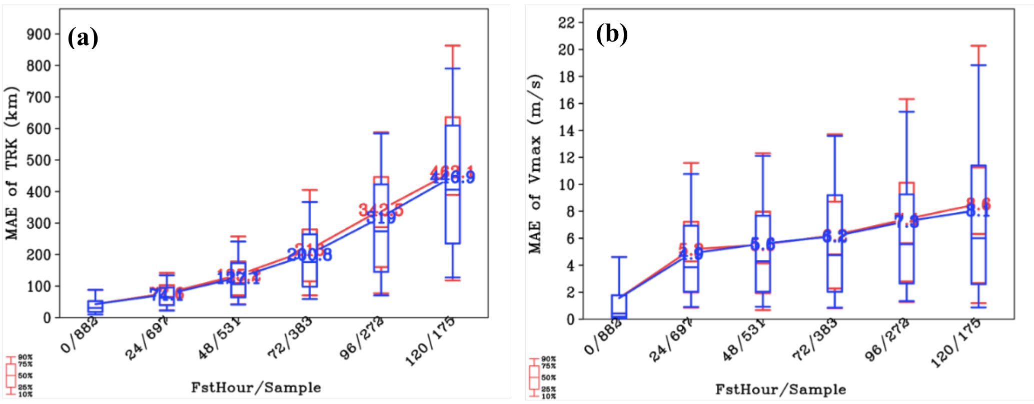

Fig. 2.2 The forecast (a) track and (intensity) errors for CMA-TYM V3.1 (red) and CMA-TYM V3.2 (blue).

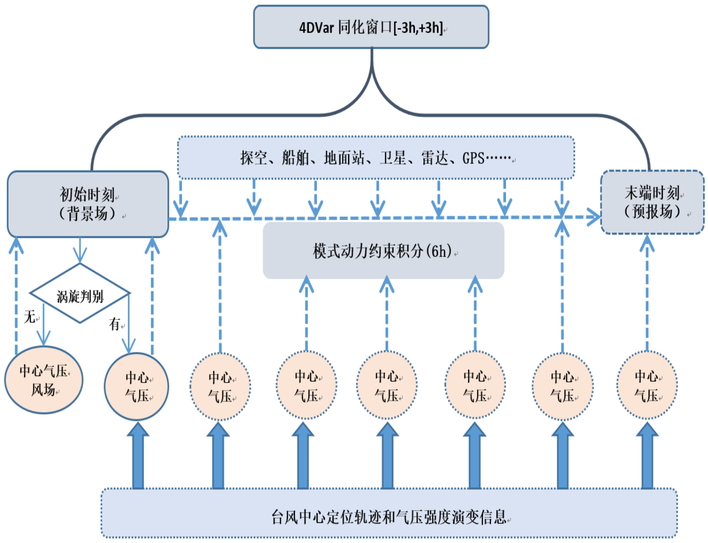

Fig. 2.3 The initialization scheme for assimilation of TC track and intensity information.

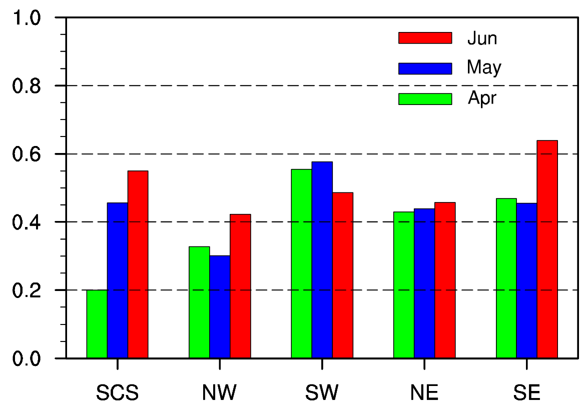

Fig. 2.4 Anomaly correlation coefficient between TC track density and observations in west Northern Pacific and the South China Sea from July to September with different lead time (the green, blue and red bar charts in the figure represent the reporting results of the model in April, May and June respectively; the horizontal axis SCS is the South China Sea, and NW, SW, NE and SE represent the four quadrants of the west Northern Pacific bounded by 140°E and 20°N).

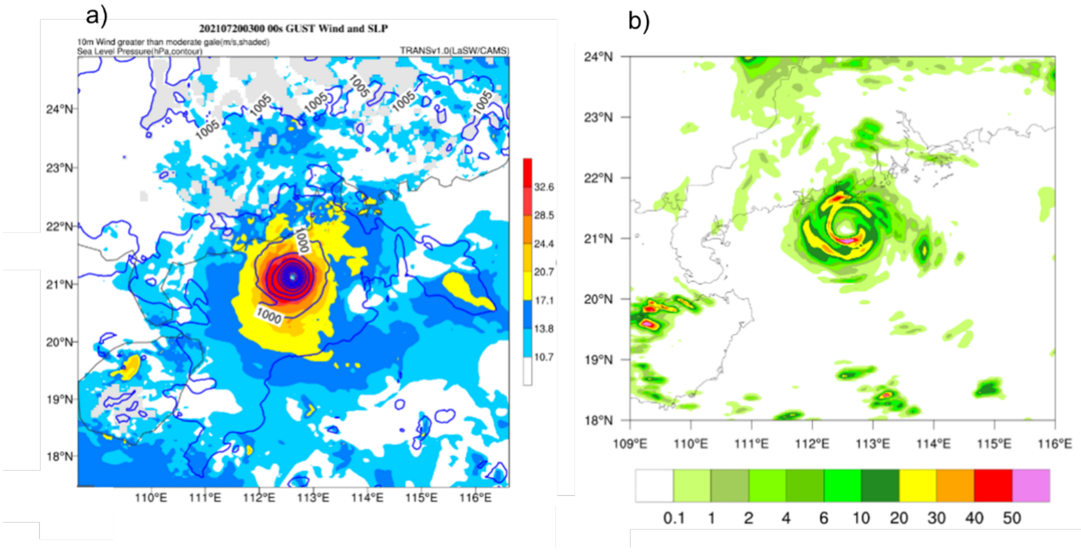

Fig. 2.5 The (a) gust and (b) rain rate prediction product of TRANSv1.0 for CEMPAKA (2021). The initial time of the forecast is 2100UTC 19 July. The forecast time of this figure is 0300UTC 20 July.

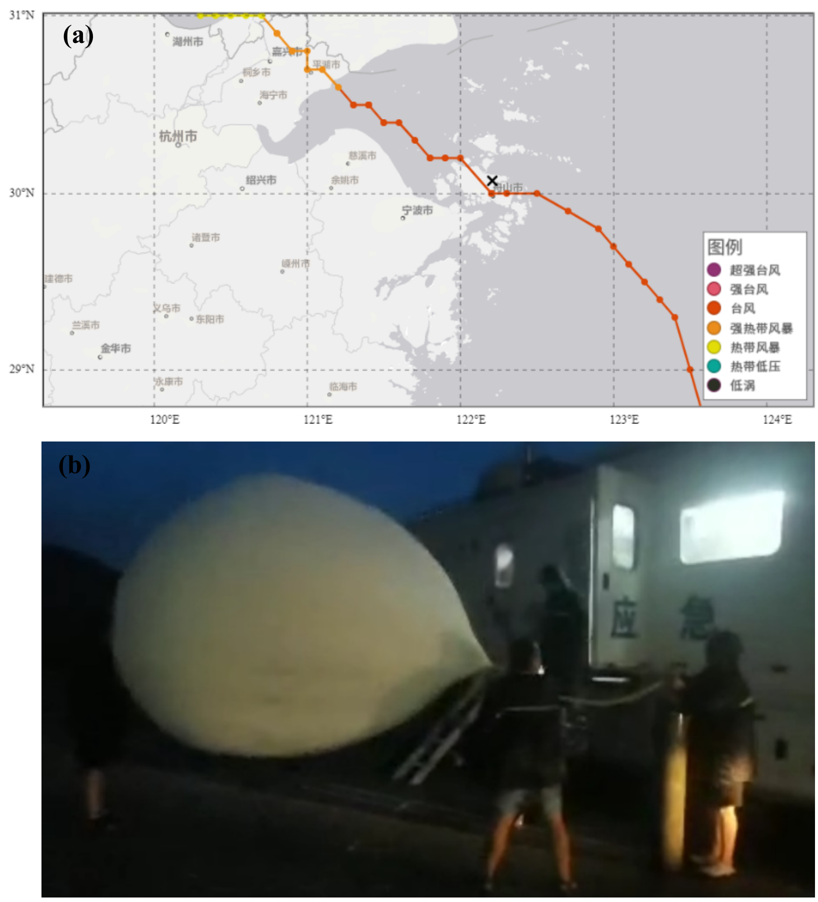

Fig. 2.6 (a) Severe Typhoon IN-FA (2106) field experiment location (× represents the location), (b) meteorological elements detection balloon.

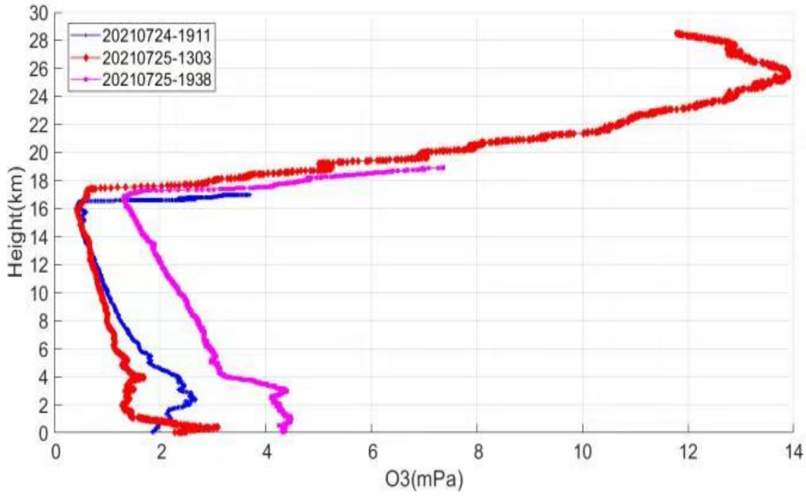

Fig. 2.7 Ozone profile of Severe Typhoon IN-FA (2106) before and after the landfall.

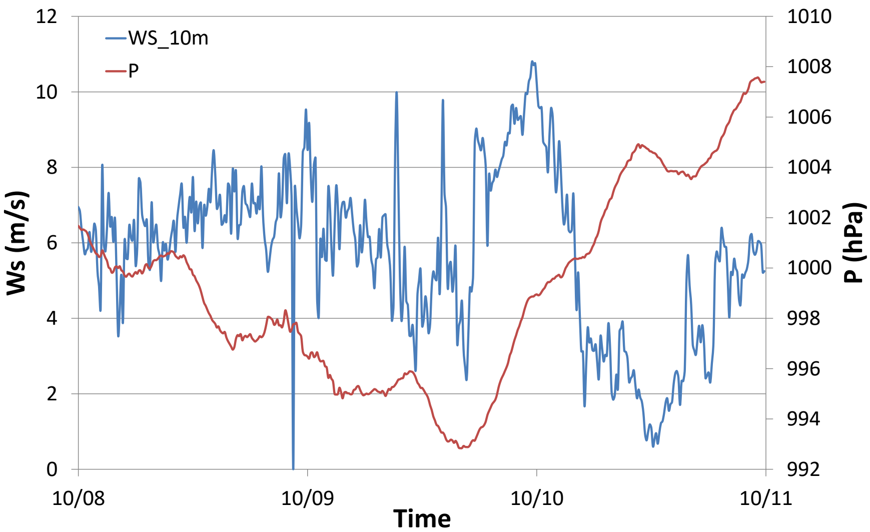

Fig. 2.8 Tropical storm LIONROCK (2117) pressure and 10m wind speed observed by Xuwen Marine Meteorological Scientific Experimental Base in Zhanjiang, Guangdong Province.

Fig. 2.9 The workshop on forecast review of Severe Typhoon IN-FA (2106) on 16 September, 2021

Fig. 2.10 The workshop on forecast review of Super Typhoon CHANTHU (2114) on 15 November, 2021

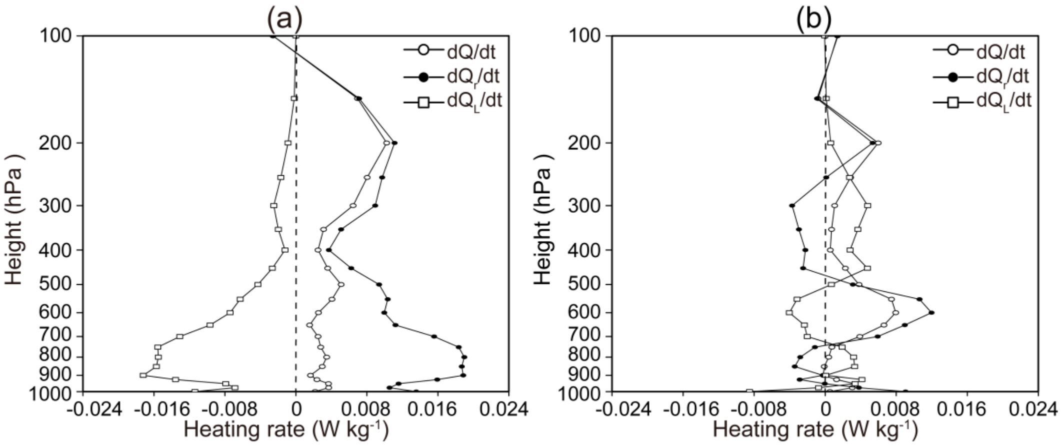

Fig. 2.11 Diabatic heating-rate difference between (a) TY1 and TY2 stages in a developing case and (b) TD1 and TD2 stages in a nondeveloping case. Values are based on averages in the square box method

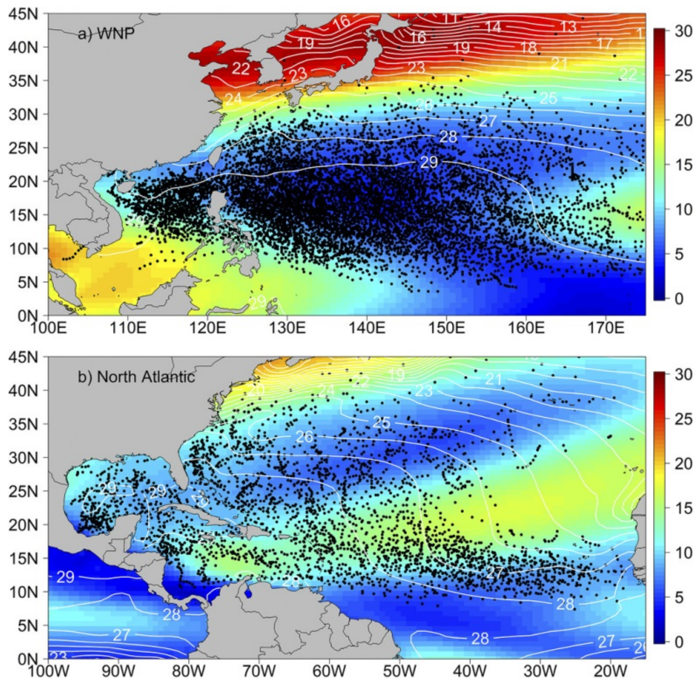

Fig. 2.12 Distribution of SST (°C; contours) and VWS (shading) averaged during June–October between 1982 and 2015 based on the monthly data over the (a) western North Pacific Ocean and (b) the North Atlantic. Dots indicate the locations of intensifying TC cases during the same season.

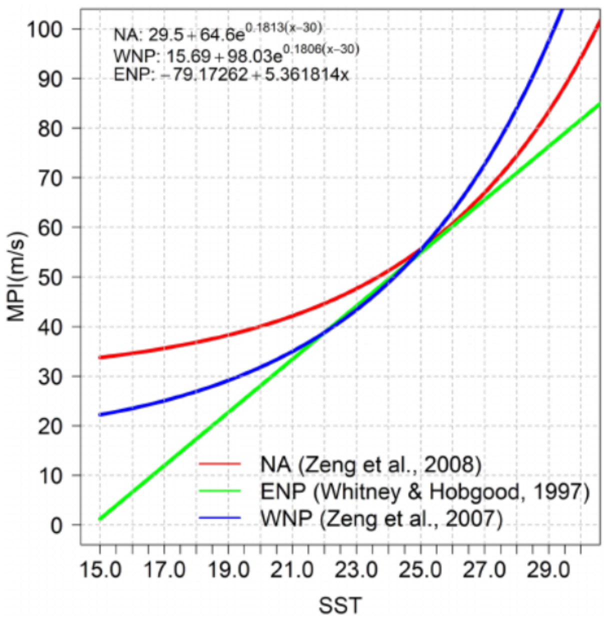

Fig. 2.13 The empirically fitted MPI as a function of SST in the North Atlantic (NA, red), eastern North Pacific (ENP, green), and western North Pacific (NWP, blue), respectively.

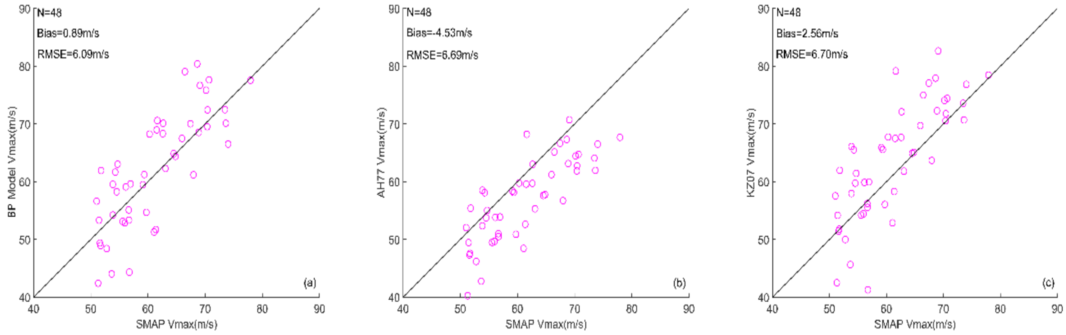

Fig. 2.14 Comparison results between the MWS of SMAP and the MWS simulated by (a) the BP neural network (Network-1) combined with Equation (8), (b) the AH77 model (Equation (2)), and (c) the KZ07 model (Equation (4)). The abscissa stands for the MWS from SMAP, and the ordinate is the simulated MWS. The number of samples (N), deviation (Bias), and RMSE of each comparison result are marked at the top of each panel.

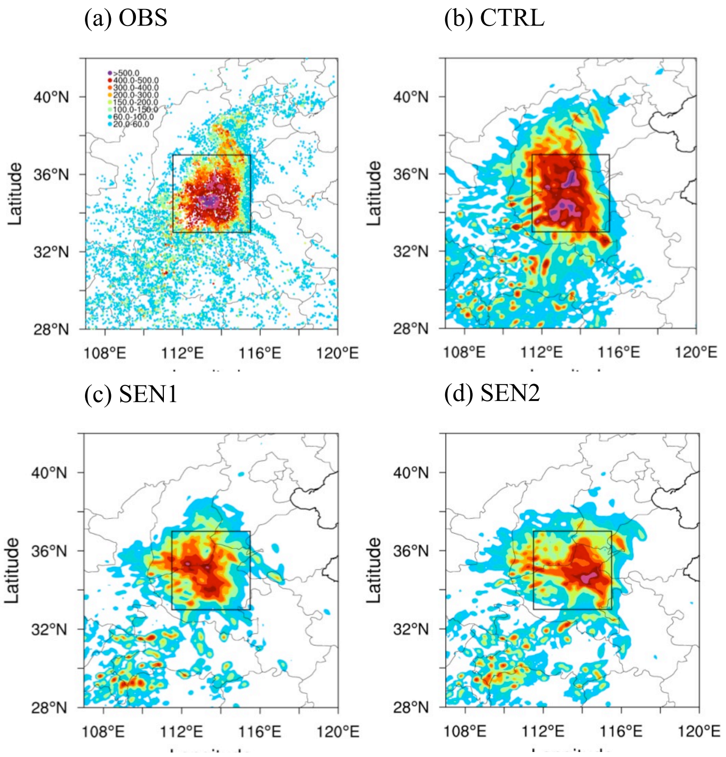

Fig. 2.15 54-h accumulated precipitation from 0000UTC 19 July to 0600UTC 21 July 2021 from the rain gauge and simulations. The black solid square denotes the targeted area in which the simulated rainfall data is compared with the observation.

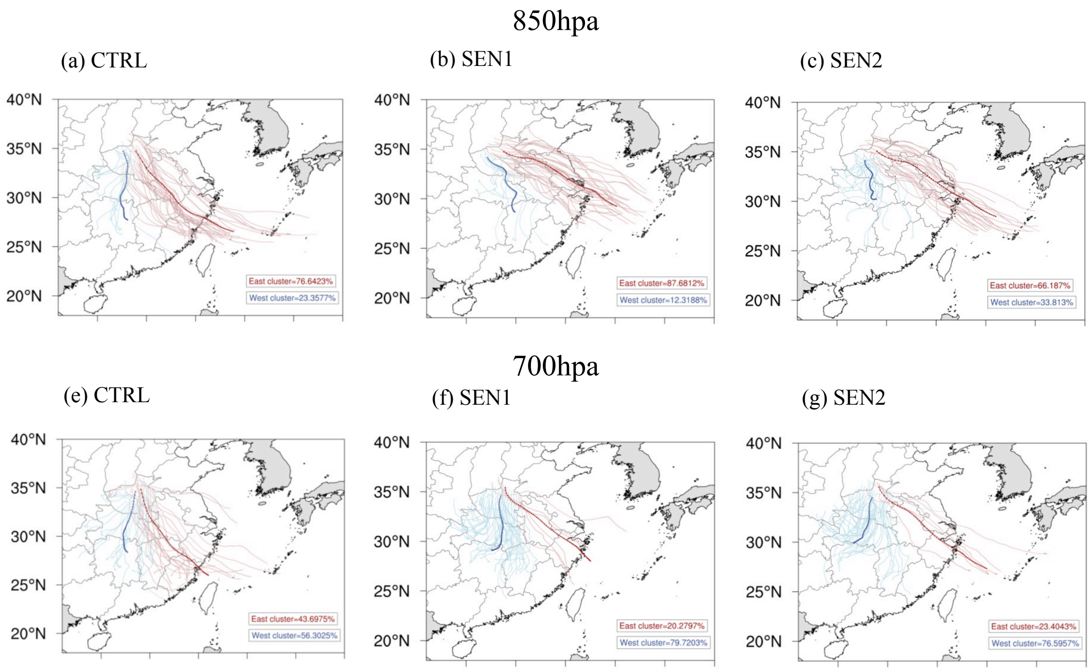

Fig. 2.16 60-h back trajectories of air parcels selected in the targeted area from the CTRL and sensitive runs. Started from 1800UTC 20 July 2021 (in the middle of stage II), 144 air parcels are released at 850hpa and 700hpa and around 48 trajectories are shown for clarity. The trajectories in blue and red

color belongs to west and east cluster and the percentage that shown at the right bottom of the figures means the proportion of the trajectories that belong to each cluster.

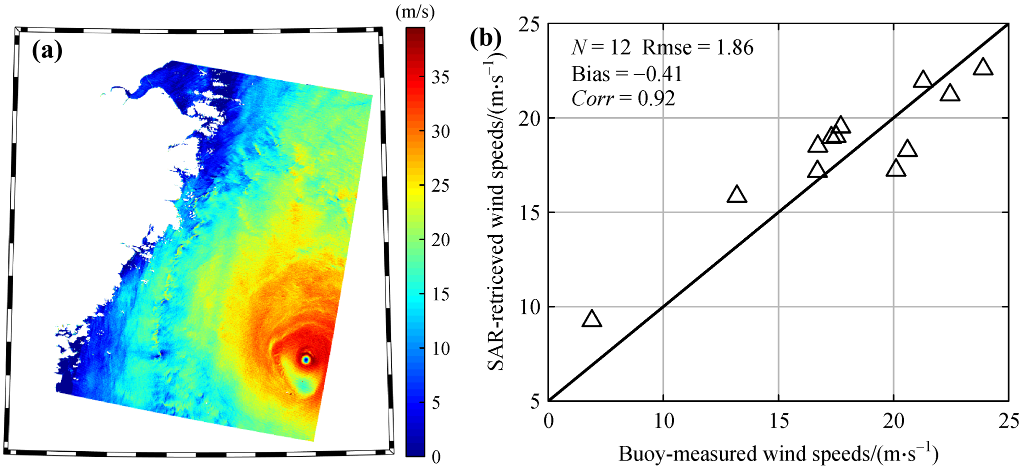

Fig. 2.17 (a) Ocean surface wind speed retrieved from the GF-3 SAR image using the QPS-CP model at VH-polarization for Super Typhoon LEKIMA (2019). (b) Ocean surface wind speeds retrieved from the GF-3 SAR image vs in situ buoy measurements.

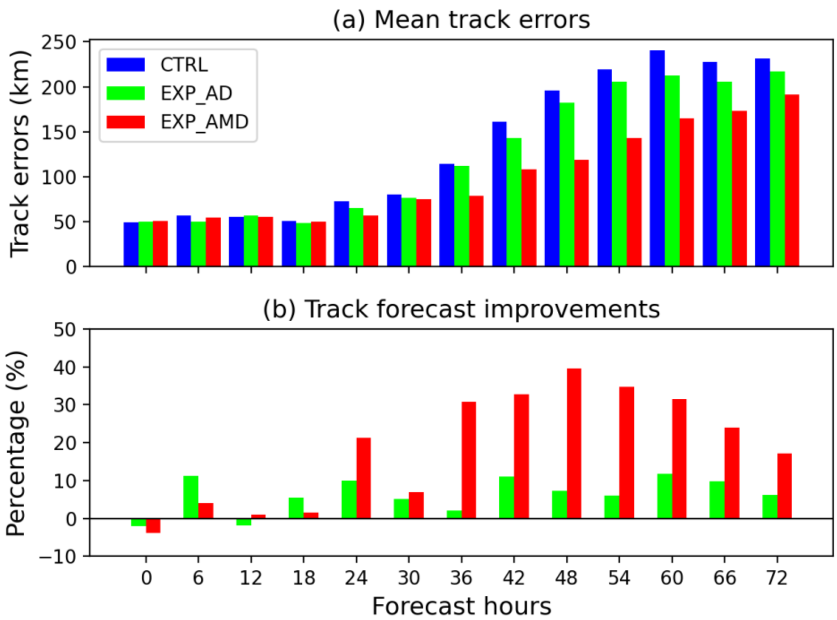

Fig. 2.18 Hindcast for LEKIMA, (a) Mean track errors (unit: km) calculated by averaging track errors of eight different initial times and (b) mean track forecast improvement (unit: %) relative to the CTRL (blue) for EXP_AD (green) and EXP_AMD (red). The x-axis represents the forecast hours.

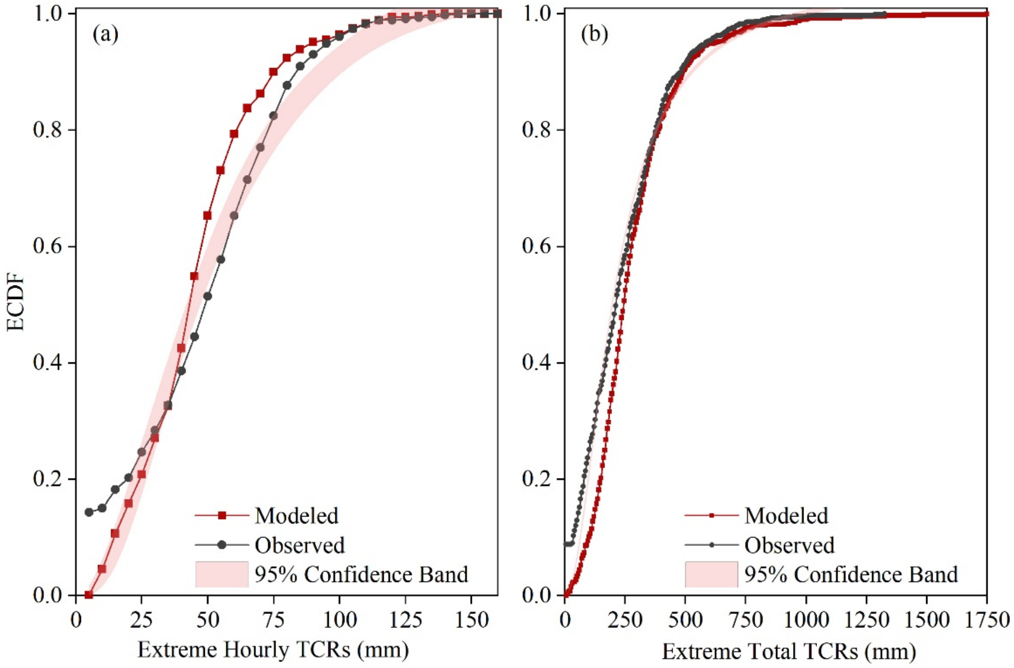

Fig. 2.19 Empirical cumulative distribution function (ecdf) for extreme hourly TCRs (a) and extreme total TCRs (b) of observed (black lines) and modeled (red lines) TCs landing in China during 1960-2018. Red shadow represents the 95% confidence band.